

# Optical linearities and size quantization in porous silicon

N. V. Gushchina, V. S. Dneprovskii, E. Yu. Dovydenko, V. A.

Karavanskii,  
and D. K. Okorokov

*Institute of General Physics, Russian Academy of Sciences, 117942 Moscow, Russia*

(Submitted 13 September 1994)

*Zh. Eksp. Teor. Fiz.* **106**, 1830–1838 (December 1994)

We have recorded bleaching bands in the nonlinear transmission spectra of porous silicon which were obtained at different times after excitation with an ultrashort laser pulse. The increase in transmission at discrete frequencies is explained by saturation of optical transitions between size-quantization levels in the system of charge carriers which are spatially localized in quasi-one-dimensional structures (quantum wires) and quasi-zero-dimensional structures (quantum dots). The results of independent measurements performed with a transmission electron microscope confirm that quantum wires and quantum dots with the corresponding sizes are present in the samples. Carriers were observed to pass from the upper to the lower size-quantization energy levels more slowly than intraband relaxation in a single crystal. © 1994 American Institute of Physics.

## 1. INTRODUCTION

Silicon, which is widely employed in microelectronics, has been attracting attention in recent years because of its potential applications in optoelectronics—primarily the possibility of obtaining visible-range radiation at room temperature from a porous structure prepared from crystalline silicon by electrochemical etching.<sup>1</sup> In spite of much experimentation, the nature of this luminescence is still not completely understood. Essentially only two alternative mechanisms have been proposed for the efficient luminescence of porous silicon (PS): a) the displacement of the luminescence spectrum into the visible region and the high luminescence efficiency are associated with a quantum-size effect (optical transitions in nanometer size structures) and b) the luminescence source is silicon compounds, for example, siloxane, which are present on the extended surface of porous silicon. The results of the latest experiments<sup>2–7</sup> apparently support the quantum-size model, but a number of experiments still cannot be satisfactorily explained. At the present time there are virtually no data which would permit determining for porous silicon the discrete energy spectrum associated with size quantization. Lamentably, the linear optical absorption spectra of porous silicon, which are shifted to shorter wavelengths than those of bulk silicon, have no features associated with the discrete energy spectrum of nanostructures. This is also true of optical excitation and reflection spectra. The absence of discrete structure in the spectra could be due to inhomogeneous broadening of optical transitions as a result of large size dispersion and different shapes of the nanostructures which comprise the porous silicon.

In the present work, we employed the method of picosecond laser saturation spectroscopy to determine the energy spectrum of samples of porous silicon.<sup>1</sup> The recorded increase of transmission at discrete frequencies suggested that the experimental samples of porous silicon contain two types of nanostructures: quantum wires and quantum dots. This was confirmed by additional measurements performed with a transmission electron microscope. Analysis of the changes in

the nonlinear transmission spectra of cooled (80 K) samples of porous silicon as a function of time made it possible to observe a transition from the upper to the lower size-quantization levels which is slow compared to intraband carrier relaxation in bulk semiconductors.

## 2. EXPERIMENTAL RESULTS

We used free films of porous silicon, which make it possible to perform measurements in transmitted radiation. Standard low-resistance KES0.01 <111> silicon (*n*-type, antimony-doped, resistivity 0.01 Ω·cm) substrates were used to prepare the films. The films were formed by anodic etching in a two-chamber teflon cell with platinum electrodes and a transmission window for additional irradiation. An electrolyte, based on a 1:1 (by volume) solution of 49% hydrofluoric acid in ethanol, was used. The anodization was conducted in two stages: a) formation of a film in the dark during a period of 30 min—current density of 7 mA/cm<sup>2</sup> and b) removal of the film from the substrate—the current density increased briefly to 100 mA/cm<sup>2</sup> under illumination by scattered light from an incandescent lamp. The irradiation conditions were chosen so as to reduce the scattering in the film to a minimum and still obtain luminescence from the films. The samples obtained consisted of 20–30 μm thick transparent plane-parallel films.

Besides nonlinear picosecond saturation spectroscopy, we employed electron microscopy, Raman scattering (RS), and photoluminescence (PL).

Images were obtained with a Philips CM30/STEM transmission electron microscope operating at a voltage of 300 keV.

The Raman-scattering and photoluminescence spectra were obtained with excitation by the 457.9 nm line of an argon laser with a power density of 1–10 W/cm<sup>2</sup>. At these power densities the thermal shift of the Raman-scattering spectra was below the resolution of the spectral system employed for recording the spectra.

The photoluminescence and Raman scattering spectra of the experimental porous-silicon film are displayed in Figs. 1 and 2. For comparison, the Raman-scattering spectrum of the

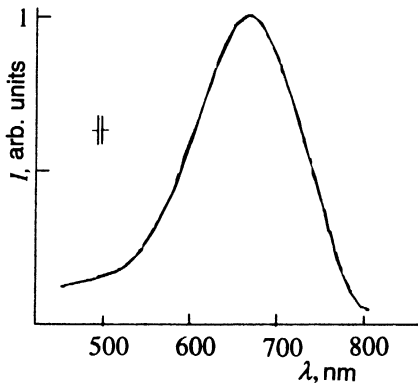


FIG. 1. Luminescence spectra of a porous-silicon sample. The spectral resolution is 2 nm.

initial substrate is also displayed in Fig. 2. The photoluminescence spectrum has the standard form, as in most published works (see, for example, Refs. 2 and 6). The maximum of the wide photoluminescence band lies near 660 nm. The Raman-scattering spectrum of porous silicon is appreciably broadened (the width is  $11 \text{ cm}^{-1}$ ) and shifted toward lower frequencies (the maximum lies at  $517 \text{ cm}^{-1}$ ) compared to the spectrum of the initial bulk silicon substrate ( $4.5 \text{ cm}^{-1}$  and  $521 \text{ cm}^{-1}$ , respectively). We note that there is no contribution from the amorphous phase (usually a wide band with a maximum at  $480 \text{ cm}^{-1}$ ). Most authors associate the shift and the broadening of the Raman-scattering spectrum of porous silicon to size limitation of the phonons in the crystalline structural elements comprising the porous-silicon framework. The magnitudes of the shift and the broadening are related to one another and are determined by the sizes and shape of the structural elements as well as the form of the correlation function and the boundary conditions, whose choice is not strictly determined.<sup>9</sup> Our results can be explained (see Ref. 10, Fig. 3) by assuming that the sample contains both spherical particles 5–7 nm in diameter and cylindrical fibers 2.0–2.5 nm in diameter.

No features indicating discrete optical transitions were observed, even at liquid-nitrogen temperatures, in the shifted

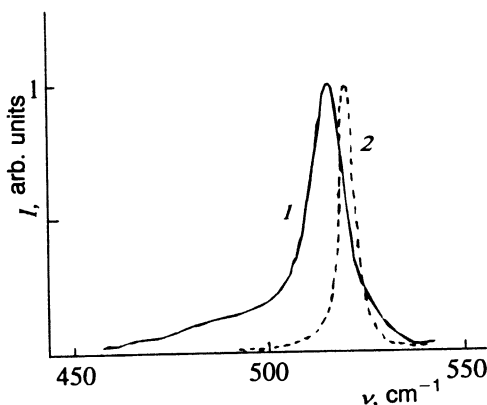


FIG. 2. Raman-scattering spectrum of a porous-silicon film (1) and the initial substrate (2). The spectral resolution is  $2 \text{ cm}^{-1}$ .

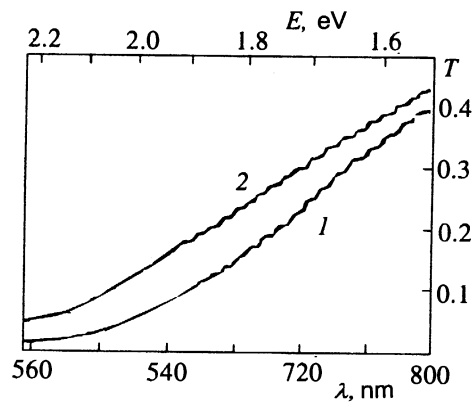


FIG. 3. Linear transmission spectra of a porous-silicon sample at 300 K (1) and 80 K (2).

(toward shorter wavelengths compared to the transmission spectra of bulk silicon) linear transmission spectra of the experimental porous-silicon films (Fig. 3). The distances between the maxima in the interference structure (the faces of the films are plane-parallel) made it possible to determine the linear index of refraction of the porous-silicon samples:  $n_0 \approx 1.9$  (for bulk silicon  $n_0 \approx 3.44$  is found<sup>11</sup>).

We note that the linear transmission spectrum of cooled porous-silicon samples (80 K) is shifted toward shorter wavelengths compared to the 300 K spectrum (Fig. 3). This shift can apparently be explained by the temperature-dependence of the band gap (in bulk silicon  $\Delta E_g^T \approx 0.03 \text{ eV}^{12}$ ).

To investigate the dynamics of nonlinear absorption, the porous silicon samples were excited with ultrashort pulses (USPs) of the second harmonic radiation of a Nd:YAG laser (the pulse duration is about 20 ps and the photon energy is 2.33 eV) and probed with an ultrashort pulse of “white” light at different times after the action of the pump pulse (an optical delay line was employed). The differential transmission spectra were calculated from the measurements of the nonlinear transmission.<sup>8</sup>

$$DT(\lambda) = \frac{T(\lambda) - T_0(\lambda)}{T_0(\lambda)}, \quad (1)$$

where  $T(\lambda)$  and  $T_0(\lambda)$  are the transmission spectra of the excited and unexcited sample. The measurements were performed at both room and liquid-nitrogen temperatures.

Figures 4 and 5 display the  $DT(\lambda)$  spectra for different delays  $\Delta t$  between the ultrashort excitation and probe pulses for sample temperatures of 300 K and 80 K. The distinctive features of the  $DT(\lambda)$  spectra is that they manifest discrete structure which does not occur in the linear transmission spectra.

Three bleaching bands were recorded at room temperature in the differential transmission spectra  $DT(\lambda)$ :  $\lambda_1 = 760 \text{ nm}$ ,  $\lambda_2 = 680 \text{ nm}$ , and  $\lambda_3 = 570 \text{ nm}$ . The  $\lambda_3$  band vanished and the amplitude of the  $\lambda_1$  and  $\lambda_2$  bands decreased considerably 30 ps after the USP.

The  $DT(\lambda)$  spectra of cooled samples of porous silicon (80 K) contained bleaching bands with maxima at the fol-

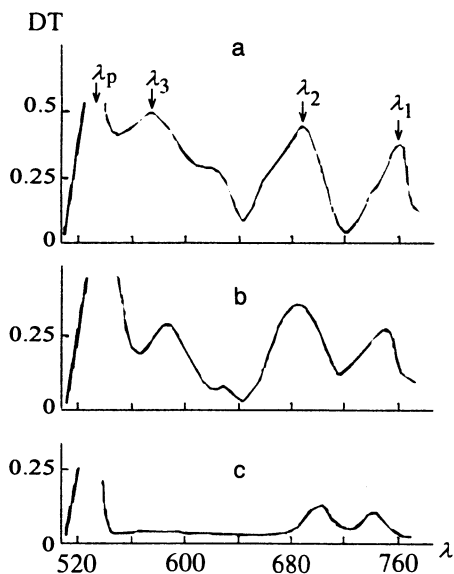


FIG. 4. Differential transmission spectra of a porous-silicon sample (at 300 K) for different delays  $\Delta t$  between the ultrashort excitation and sounding pulses:  $\Delta t=0$  (a), 20 (b), and 27 ps (c).

lowing wavelengths:  $\lambda'_1=730$  nm,  $\lambda'_2=670$  nm,  $\lambda'_3=630$  nm,  $\lambda'_4=590$  nm,  $\lambda'_5=565$  nm.

The amplitudes of the  $\lambda'_2$ ,  $\lambda'_3$ , and  $\lambda'_5$  bands decreased monotonically as the delay between the ultrashort excitation and sounding pulses increased. The amplitudes of the  $\lambda'_1$  and  $\lambda'_4$  bands with delay times  $\Delta t \leq 10$  ps increased and then also decreased. All bleaching bands vanished almost completely after 30 psec.

The decrease in the number of bleaching bands at room temperature can be attributed to thermal broadening and

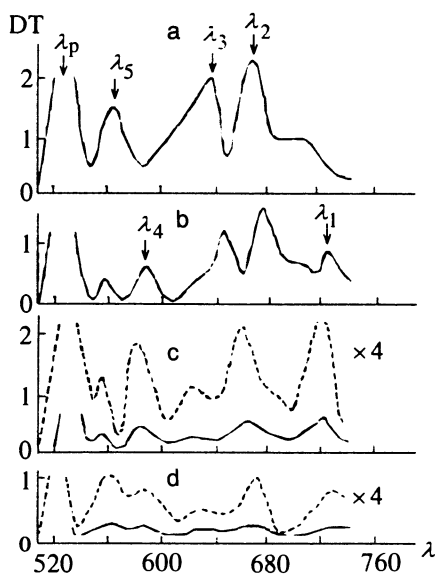


FIG. 5. Differential transmission spectra of a porous-silicon sample (at 80 K) with different delays  $\Delta t$  between the ultrashort excitation and sounding pulses:  $\Delta t=0$  (a), 10 (b), 13 (c), and 27 ps (d).

merging of the  $\lambda'_4$  and  $\lambda'_5$  bands into the  $\lambda_3$  band and of the  $\lambda'_2$  and  $\lambda'_3$  bands into the  $\lambda_2$  band.

### 3. DISCUSSION OF THE EXPERIMENTAL RESULTS

The absence of discrete structure in the linear-transmission spectra is probably explained by the strong inhomogeneous broadening of the size-quantization levels as a result of both the large spread of the sizes of the nanocrystals and the transverse sizes of the thin filaments and the different shapes of these structures. This broadening is probably largely suppressed in the nonlinear transmission spectrum because the carriers in structures of definite size are selectively excited by the narrow-band pumping radiation. The carriers are most efficiently excited in nanocrystals and filaments whose transverse size is such that the energy of an optical transition is close to the energy of a pump photon. This effect was observed previously in Ref. 13 and analyzed in Ref. 14. The features of the differential transmission spectra (Figs. 4 and 5) can apparently be attributed to the saturation of optical transitions in the system of carriers, which are localized in quasi-one-dimensional and quasi-zero-dimensional structures, under optical excitation.<sup>15</sup>

To estimate the energies of the optical transitions in porous silicon, we assumed that the fibers are long parallelepipeds oriented in the [001] direction, which is assumed to be the predominant direction during pore growth.<sup>16</sup> The parallelepipeds are assumed to have a square cross section with faces perpendicular to the [110] and  $[1\bar{1}0]$  directions.

To get an idea of the character of the optical transitions in porous silicon, in Ref. 17 it was proposed to study the projection of the band structure of the bulk material on the one-dimensional Brillouin zone of a quantum wire. In this case, two electronic valleys, lying in the [001] direction, form an indirect minimum (with  $k \approx 0.4\pi/a$ ). Four electronic valleys are projected into the center of the Brillouin zone and form a direct minimum.<sup>18</sup>

In this case, the energies of the optical transitions can be estimated according to the formula

$$E = E_g + \frac{\hbar^2 \pi^2}{2\mu_{h(l)} L^2} (n_1^2 + n_2^2), \quad (2)$$

where  $E_g$  is the band gap in bulk silicon;  $\mu_{h(l)} = m^e m_{h(l)}^h / (m^e + m_{h(l)}^h)$  is the reduced mass of the carriers, taking into account heavy (h) and light (l) holes;  $m^e = m_{\perp}^e m_{\parallel}^e / (m_{\perp}^e + m_{\parallel}^e)$  is the reduced electron mass ( $m_{\perp}^e = 0.19m_0$  and  $m_{\parallel}^e = 0.92m_0$  are, respectively, the transverse and longitudinal electron masses.<sup>11</sup>;  $L$  is the transverse size of a quantum wire; and  $n_1$  and  $n_2$  are quantum numbers ( $n_{1,2} = 1, 2, 3, \dots$ ).

The  $\lambda_1$  and  $\lambda_2$  bands in the 300 K differential transmission spectra  $DT(\lambda)$  can be explained by saturation of the optical transitions between two lower size-quantization levels  $E_{11}^h$  and  $E_{11}^l$  in the quantum wires. Using the expression (2) the transverse size of the wires was estimated from the short-wavelength shift of the  $\lambda_1$  and  $\lambda_2$  bands relative to  $E_g$  to be 2.7–3.3 nm.

The positions of the  $\lambda'_1$  and  $\lambda'_2$  bands in the  $T=80$  K differential transmission spectra can be explained by satura-



FIG. 6. Image of the structure of different sections of a porous-silicon film. The images were obtained with a transmission electron microscope: a) thin filaments (quantum wires) and b) nanocrystals (quantum dots).

tion of the optical transitions between two lower size-quantization levels  $E_{11}^h$  and  $E_{11}^l$  in the quantum wires. The transverse size of the wires in this case is 2.8–3.4 nm. The  $\lambda_3'$  transmission band probably also corresponds to the lower optical transition  $E_{11}^h$ , but for wires with a transverse size of 2.5 nm. In this case, the transition energy  $E_{11}^l$  equals the pump energy (2.33 eV).

It is clear from the foregoing discussion that wires with a transverse size of 2.7–3.4 nm make the main contribution to the optical nonlinearities. The reason for this is that apparently the energy  $E_{12}^h(E_{21}^h)$  of the third optical transition corresponding to this size is close to the energy of the laser pump photon ( $\hbar\omega_p = 2.33$  eV). It is because these energies are so close that the interaction with the incident radiation is highly efficient.

The positions of the  $\lambda_4'$  and  $\lambda_5'$  bands in the spectrum cannot be explained by saturation of the optical transitions between the next size-quantization levels  $E_{12}^{h(1)}$  and  $E_{21}^{h(1)}$  of quantum wires with transverse sizes of 2.5–3.0 nm. It is natural to conjecture that these porous-silicon samples contain, besides thin wires, nanocrystals (quantum dots). It can then be conjectured that the  $\lambda_4'$  and  $\lambda_5'$  bands are associated with the saturation of the transitions between lower energy levels of carriers located in the nanocrystals. In this case, the energies of the optical transitions can be estimated (we neglect the Coulomb interaction of the carriers and assume that the nanocrystals are spherical) according to the formula<sup>19</sup>

$$E_{l,n} = E_g + \frac{\hbar^2 \varphi_{l,n}^2}{2\mu_{h(l)} R^2}, \quad (3)$$

where  $\varphi_{l,n}$  is the  $n$ th root of a Bessel function of half-integer order  $(l+1/2)$ ,  $l$  is the angular momentum,  $\mu_{n(l)} = m^e m_{h(l)}^h / (m^e + m_{h(l)}^h)$  is the reduced mass, and  $R$  is the average radius of the quantum dots. The average radius of the nanocrystals in this case is 2.0 nm.

The existence of both types of nanostructures was confirmed by independent measurements performed with a transmission electron microscope. Figures 6a and b display images of different parts of the experimental porous-silicon film. These images were obtained with the electron beam transmitted perpendicularly through the surface of the film (the initial substrate was oriented in the  $\langle 111 \rangle$  direction). Naturally, an image can be obtained only at the edges of the films (in the region of thin slices). The structure of the porous-silicon sample is similar to a sponge consisting of thin filaments and small particles of different shape and substantial size variation. The filaments are oriented in different directions and their transverse sizes range from 2 to 10 nm. The spread in the sizes of the small particles is approximately the same as for the filaments.

As noted above, the amplitude of the  $\lambda_1'$  and  $\lambda_4'$  bleaching bands in the cooled (80 K) porous-silicon samples increases as the delay between the pump and sounding pulses increases up to 10 ps. It is natural to associate the increase of bleaching to an increase of the population of the lower size-quantization levels of quantum wires and quantum dots as a result of carrier-relaxation from the upper size-quantization energy levels. This relaxation process is slower than intraband relaxation in bulk silicon. The slowing down of the relaxation in quasi-one-dimensional and quasi-zero-dimensional structures could be one reason why the radiative-recombination efficiency decreases.<sup>20</sup> The decrease in the amplitude of the transmission bands was apparently determined by carrier recombination.

The imaginary part of the Kerr nonlinear cubic susceptibility in the spectral range  $\lambda = 680\text{--}730$  nm (region of the absorption edge) can be estimated from the obtained experimental data. In the case of relatively low carrier densities  $N$ , when higher-order nonlinear susceptibilities can be neglected, this quantity can be estimated from the expression

$$\text{Im } \chi^{(3)}(\omega) = \frac{c^2 n_0^2}{8 \pi^2 \omega} \frac{\tau \alpha_0(\omega) \Delta \alpha(\omega)}{\hbar \omega N}, \quad (4)$$

where  $\tau$  is the characteristic carrier lifetime and  $\Delta \alpha(\omega)$  is the change in the absorption. Substituting the measured values of  $\Delta \alpha(\omega)$  and  $\tau$ , we obtain  $\text{Im} \chi^{(3)} \approx 0.2 \cdot 10^{-8}$  cgs (300 K) and  $\text{Im} \chi^{(3)} \approx 0.7 \cdot 10^{-8}$  cgs (80 K). Therefore, the nonlinear susceptibility of porous silicon is higher than that of nanocrystalline materials with close relaxation times<sup>21</sup> but much lower than the resonance nonlinear susceptibilities of bulk direct-band semiconductors.<sup>22</sup> This latter circumstance is associated with the low content of the porous structure and relaxation times substantially lower than those of the bulk semiconductors. Moreover, apparently, the inhomogeneous broadening of the energy levels has a considerable effect: As a result of this homogeneous broadening, only a small fraction of the nanostructures participates in the formation of the nonlinear-optical response.

In conclusion, we note that picosecond laser saturation spectroscopy allowed us to record saturation of discrete optical transitions in porous silicon and to determine the size-quantization energy spectrum of two types of nanostructures: nanocrystals (quantum dots) and thin filaments (quantum wire). The quantum character of the optical transitions is confirmed by the observed slowing down of the relaxation of the energy of the photoexcited carriers in porous silicon compared to intraband relaxation in a bulk semiconductor. In addition, we were able to observe the existence of both types of nanostructures with the corresponding sizes in the experimental samples of porous silicon by performing measurements with a transmission electron microscope. The obtained high values of the rapidly relaxing nonlinear cubic susceptibility of porous crystal show that such crystals are promising for optical switching.

This work was performed with financial support from the Russian Fund for Fundamental Research (project 93-02-2214), the International Science Fund (grant No. M5D000), and the program "Physics of solid-state nanostructures" (projects 1-034 and 1-042).

<sup>1)</sup>The discrete nonlinear-transmission spectrum of porous silicon was discovered by Dneprovskii *et al.*,<sup>8</sup> who explained it by saturation of optical transitions between size-quantization levels in quasi-one-dimensional structures.

<sup>1</sup> L. T. Canham, *Appl. Phys. Lett.* **57**, 1046 (1990).

<sup>2</sup> M. Enachescu, E. Hartman, and F. Koch, *Appl. Phys. Lett.* **64**, 1365 (1994).

<sup>3</sup> R. F. Pinizzitto, H. Yang, J. M. Perez, and J. L. Coffey, *J. Appl. Phys.* **75**, 4486 (1994).

<sup>4</sup> O. Teschke, F. Alvares, L. Tessler, and M. V. Kleinke, *Appl. Phys. Lett.* **63**, 1927 (1993).

<sup>5</sup> M. Koos, I. Pocsik, and E. B. Vazsonyi, *Appl. Phys. Lett.* **62**, 1797 (1993).

<sup>6</sup> S. L. Friedman, M. A. Marcus, D. L. Adler *et al.*, *Appl. Phys. Lett.* **62**, 1934 (1993).

<sup>7</sup> K. Inoue, K. Maehashi, and H. Nakashima, *Jpn. J. Appl. Phys.* **32**, L631 (1993).

<sup>8</sup> V. S. Dneprovskii, V. A. Karavanskii, V. I. Klimov, and A. P. Maslov, *Pis'ma Zh. Eksp. Teor. Fiz.* **57**, 394 (1983) [*JETP Lett.* **57**, 406 (1993)].

<sup>9</sup> H. Richter, Z. P. Wang, and L. Ley, *Solid State Commun.* **39**, 625 (1981).

<sup>10</sup> I. I. Reshina and E. G. Guk, *Fiz. Tekh. Poluprovodn.* **27**, 732 (1983) [*Sov. Phys. Semicond.* **27**, 401 (1993)].

<sup>11</sup> Landolt-Bornstein, *Numerical Data and Functional Relationships in Science and Technology*, **17a**, 70, Springer, Berlin, 1982.

<sup>12</sup> M. Voos, P. Uzan, C. Delalande, G. Bastard, and A. Halimaoui, *Appl. Phys. Lett.* **61**, 1213 (1992).

<sup>13</sup> Yu. V. Vandyshchev, V. S. Dneprovskii, and V. I. Klimov, *Zh. Eksp. Teor. Fiz.* **101**, 270 (1982) [*Sov. Phys. JETP* **74**, 144 (1992)].

<sup>14</sup> V. I. Klimov, *Fiz. Tverd. Tela* **34**, 2472 (1992) [*Sov. Phys. Solid State* **34**, 1326 (1992)].

<sup>15</sup> S. Schmitt-Rink, D. A. B. Miller, and D. S. Chemla, *Phys. Rev. B* **35**, 8113 (1987).

<sup>16</sup> R. L. Smith and S. D. Collins, *J. Appl. Phys.* **71**, R1 (1992).

<sup>17</sup> G. D. Sanders and Y.-C. Chang, *Phys. Rev. B* **45**, 9202 (1992).

<sup>18</sup> F. Buda, J. Kohanoff, and M. Parrinello, *Phys. Rev. Lett.* **69**, 1272 (1992).

<sup>19</sup> A. L. Éfros and A. L. Éfros, *Fiz. Tekh. Poluprovodn.* **16**, 1209 (1992) [*Sov. Phys. Semicond.* **16**, 772 (1982)].

<sup>20</sup> H. Benisty, C. M. Sotomayor-Torres, and C. Weisbuch, *Phys. Rev. B* **44**, 10945 (1991).

<sup>21</sup> S. S. Yao, C. Karaguleff, A. Gabel *et al.*, *Phys. Lett.* **46**, 801 (1985).

<sup>22</sup> H. M. Gibbs, S. L. McCall, T. N. C. Venkatesan *et al.*, *Appl. Phys. Lett.* **35**, 35 (1979).

Translated by M. E. Alferieff